Accepted Manuscript

Binding of Clitoria ternatea L. flower extract with α-amylase simultaneously monitored at two wavelengths using a photon streaming time-resolved fluorescence approach

Graham Hungerford, M. Adília Lemos, Boon-Seang Chu

PII:	S1386-1425(18)31059-X
DOI:	https://doi.org/10.1016/j.saa.2018.11.062
Reference:	SAA 16626
To appear in:	*Spectrochimica Acta Part A: Molecular and Biomolecular Spectroscopy*
Received date:	26 July 2018
Revised date:	14 November 2018
Accepted date:	29 November 2018

Please cite this article as: Graham Hungerford, M. Adília Lemos, Boon-Seang Chu , Binding of Clitoria ternatea L. flower extract with α-amylase simultaneously monitored at two wavelengths using a photon streaming time-resolved fluorescence approach. Saa (2018), https://doi.org/10.1016/j.saa.2018.11.062

Binding of *Clitoria ternatea* L. flower extract with α-amylase simultaneously monitored at two wavelengths using a photon streaming time-resolved fluorescence approach

Graham Hungerford[1], M. Adília Lemos[2] and Boon-Seang Chu[2]

[1]*HORIBA Scientific, 133 Finnieston Street, Glasgow, G3 8HB, UK*

[2]*Division of Food and Drink, School of Science, Engineering and Technology, Abertay University, 40 Bell Street, Dundee DD1 1HG, UK.*

Abstract

The binding of an extract from the flowers of *Clitoria ternatea* L. to the digestive enzyme α-amylase was investigated. This extract is a mixture of flavonoids, including anthocyanins, and has been previously shown to inhibit the activity this enzyme. This has implications for modulating starch digestion. Since the extract contains a mixture of flavonoids, including anthocyanins, in order to investigate the kinetics, we made use of time-resolved fluorescence to simultaneously monitor two different emission bands emanating from the extract. This measurement was enabled by the use of a "photon streaming" approach and changes in fluorescence lifetime and intensity were used to follow the interaction. A longer wavelength band (655 nm) was ascribed to anthocyanins in the mixture and these were observed to bind at a rate an order of magnitude slower than other flavonoids present in the extract, monitored at a shorter wavelength (485 nm). Changes in the fluorescence emission of the extract upon binding were further assessed by the use of decay associated spectra.

Keywords

Anthocyanins; Butterfly pea; Enzyme inhibition; Flavonoids; TCSPC

Highlights

- *Clitoria ternatea* L extract inhibits α-amylase activity
- Binding monitored using time-resolved fluorescence
- Photon streaming enables simultaneous two wavelength data acquisition
- Anthocyanins bind ~10 times slower than other flavonoids

1. Introduction

The increasing incidence of chronic diseases, including type 2 diabetes, metabolic syndrome and obesity, is becoming a major health concern [1]. There is a research drive to find “natural” ways to prevent and/or manage these diseases. Plants are good sources of compounds which have been associated with health benefits, including anti-carcinogenic, anti-obesity, anti-inflammatory and anti-oxidant properties. Of particular interest are compounds such as polyphenols. There are reports that flavonoid (a class of polyphenolic compounds including anthocyanin) containing extracts from certain plant based products, such as black carrot [2], black currant [3], blue maize [4] and macqui berries [5] inhibit the digestive enzyme α-amylase. In humans α-amylase is found in saliva and pancreatic secretions [6]. It acts on polysaccharides, for example in the case of starch to give glucose [7]. The use of natural enzyme inhibitors has the potential to modulate starch digestion and, consequently, to lower the postprandial hyperglycaemic response [8,9,10]. Thus, inhibition of α-amylase using naturally occurring plant extracts has potential in the control of diabetes [8]. We have demonstrated that an extract from the flower of *C. ternatea* (commonly known as the butterfly pea) can inhibit α-amylase during starch digestion [11]. *C. ternatea* (CT) belongs to the Fabaceae family of climbing vines and its flower petals are blue-purple in colour with yellow centres. The colouration is in part related to the presence of anthocyanins, which have been found to be exceptionally stable in weak acidic or neutral conditions [12]. The extract has traditionally been used as a food colouring in South East Asia [13] and consist of a mixture of compounds. These include anthocyanins, quercetin glycosides and malonylated flavonoid glycosides [14,15,16,17]. The exact make-up of the extracted mixture is dependent on the colour of the petals, with different colour lines in addition to the wild type blue available [18]. Also on the petal to leaf ratio and extraction time have an influence [19].

Since many of the compounds in the CT extract exhibit fluorescence, we extend our previous work [11] to monitor the interaction of CT extract with α-amylase by making use of the sensitivity of time-resolved fluorescence techniques based on time-correlated single-photon counting (TCSPC) [20]. Although there are a range of compounds in the CT extract, we have found that their fluorescence emission falls within two principal spectral regions (around 485 nm and 655 nm), which can both be excited at a wavelength of 392 nm. By making use of two detectors it is possible to monitor both of these wavelengths simultaneously. The fact that two spectral regions are being simultaneously assessed is of importance as it enables a fuller picture of the binding process to be obtained and provides information that would be missed if the more usual approach of monitoring a single region was employed.

In order to make use of the fluorescence lifetime to follow the binding process we use a “photon streaming” methodology, also known as “time-tagging”. Here rather than directly building up fluorescence decay histograms, the individual photon arrival events are time-

stamped in relation to both the start of the experiment (macrotime) and in relation to the excitation pulse (microtime). It is also allows for the labelling of different detection channels. Thus, it is possible to obtain TCSPC data simultaneously using two detection channels, monitoring the emission at two different wavelengths. We have previously used a time-tag approach to monitor the gelation and changes in microenvironment in sol-gel derived media [21]. Although this methodology generates large amounts of data, it enables flexibility during the analysis to produce decay histograms at different macrotime resolutions. In the end, the time-resolution is only limited by the number of photon events in the histogram required to facilitate data analysis [22]. The use of decay associated spectra [20] also helped to elucidate the interaction between extract and enzyme.

2. Experimental

2.1 Sample preparation

Sundried *C. ternatea* (CT) flowers were obtained from a local marketplace in Penang, Malaysia. These flowers were then dried in an oven at 45 °C in the laboratory and stored in an airtight container and kept in a dark cool place until required. Lyophilised α-amylase from *Bacillus* sp. (Type II-A, ≥1,500 units / mg protein) and wheat starch were obtained from Sigma-Aldrich (Dorset, UK). The extract was obtained by soaking approximately 10 g of dry CT flower petals in 100 mL of distilled water overnight at room temperature. The solution was then filtered through doubled layer of cheesecloth and freeze-dried in an Edwards Micro Modulyo freeze-dryer (Bristol, UK). The lyophilised extract was ground into powder and a stock solution of 97.5 mg/mL in sodium phosphate buffer (SPB, 0.1 M, pH 6.9) was prepared. This was kept at –20 °C until used. For fluorescence experiments 6 μL of the stock was added to 3 mL of water to form a stock for these measurements. This was further diluted by taking 300 μL of this solution and adding to 2 mL of water in a fluorescence cuvette to make a low optical density solution for the fluorescence measurements. The final concentration of CT extract for the measurements was therefore ~30 μg / mL.

2.2 Starch digestion experiments

The starch digestion experiment has been described in detail elsewhere [11], but briefly for completeness the inhibitory effect of the extract against α-amylase during *in vitro* starch digestion was investigated as a function of CT or wheat starch concentration. The digestion of gelatinised wheat starch solution by α-amylase was performed at 37 °C, with equal starch and enzyme concentrations (1 mg / ml) used. Starch digestion was monitored via the liberation of glucose using the addition of 3,5-dinitrosalicylic (DNS) acid reagent and UV-vis spectroscopy (using a Genesys Model 6, Thermo Fisher Scientific), with the reaction monitored at 540 nm. A glucose calibration curve was run and correction made for anthocyanin absorbance.

2.3 Fluorescence measurements

Steady state fluorescence measurements were performed using a HORIBA Scientific FluoroLog-3, after initial absorption measurements made using a Shimadzu UV-1800. Time-resolved fluorescence data were obtained using a HORIBA Scientific DeltaFlex fluorimeter equipped with DeltaDiode excitation sources and two emission channels. Detection was made using two hybrid detectors (HPPD-650 and HPPD-720). The binding experiment was performed by using the (very low deadtime) timing electronics in "photon streaming" mode. This mode (also referred to as "time-tagging" or "FIFO" mode) enables the time-stamping of individual photons [21] and for simultaneous acquistion of data from both detection channels. A 3 MHz internal macrotime clock rate was used. The streamed photon arrival data was then transformed into histograms for fluorescence lifetime analysis. The EzTime analysis module has the ability to analyse >25,000 histograms. These were analysed globally as a sum of exponentials (see eq. 1), linking common lifetimes to all of the decays, using reconvolution analysis [23]. A value for the average lifetime was also returned.

The fluorescence decay is of the form

$$I(t) = \sum_{i=1}^{n} \alpha_i \exp\left(-\,t/\tau_i\right) \qquad \ldots(1)$$

With the contribution of each lifetime represented by the normalised pre-exponential (α, see eq. 2) to indicate the relative "concentration" or as a fractional or relative amplitude (*f*, pre-exponential factor weighted by the lifetime) to indicate the relative contribution to the steady state fluorescence (eq. 3)

$$\alpha_i = \frac{\alpha_i}{\sum_{i=1}^{n} \alpha_i} \qquad \ldots(2)$$

$$f = \frac{\alpha_i \tau_i}{\sum \alpha_i \tau_i} \qquad \ldots(3)$$

The average lifetime was obtained from

$$\tau_{ave} = \sum_{i=1}^{n} \alpha_i \tau_i \qquad \ldots(4)$$

Kinetic data was further treated using FluorEssence (Origin) software and smoothing applied to assist clarity. The sample was maintained at 37 °C using a Peltier (Quantum North West) equipped sample holder. Decay associated spectra were calculated from the global analysis module within the EzTime software package from a TRES (time-resolved emission spectrum) measurement. This involved the collection of decay histograms for equal data collection times at 5 nm intervals. The data were analysed as the sum of a four exponential decay, with one

lifetime fixed to half the width of a time bin (13 ps) to account for scatter and / or lifetimes beyond the time resolution of the equipment ($\tau \geq$ ~25 ps [24]).

3. Results and discussion

The absorption spectrum of the CT extract (Fig. 1(a)) exhibits bands between 500 nm and 650 nm, as well as a shorter wavelength band around 300 nm. The complexity of the extract means that it is not surprising that there are multiple emission bands (Fig. 1(b)). The longer wavelength band is most likely to derive from the anthocyanins, while the shorter wavelength band originates from flavonol glycosides [15]. An excitation wavelength of 392 nm was chosen so that both of these emissions could be obtained. This enables the simultaneous measurement of two wavelength regions (485 nm and 655 nm) in order to monitor the binding of different species present in the CT extract. The resultant fluorescence decays (see Fig 1(b)) were found to be multi-exponential, with the shorter wavelength emission exhibiting an longer-lived average lifetime. Because of the complexity of the CT extract, the lifetimes obtained are most likely a combination of different fluorescing species and, since we are not attempting to perform any separation, should be used to observe relative changes. It is also worthy of note that a spectral overlap exists between the shorter wavelength emission and the absorption of anthocyanins present in the extract. This could allow (under the appropriate circumstances) for an energy transfer (FRET) process to occur [25], although unlikely in free solution.

It has previously been shown that CT extract can inhibit the digestion of starch by α-amylase [11] and this is demonstrated in Fig. 2, where α-amylase was present at a concentration of 1 mg / mL. The inhibition appeared to be extract dose dependent and about 90 % of α-amylase inhibition was achieved with an extract concentration of 5.2 mg / mL. We have an indication that it is a competitive binding process [11], however that study only investigated the binding of anthocyanins. In order to further elucidate the interaction between the CT extract as a whole and the α-amylase the sensitivity of a time-resolved fluorescence methodology was employed. We have previously used this to investigate food related bioactive compounds [26]. In order to follow the binding kinetics a “histogram streaming” approach (also referred to as “kinetic TCSPC”) was employed. This involves the seamless collection of decay histograms, with acquisition times as short as 1 ms. This approach was used to monitor the binding of curcuminoids to serum albumin [24,26] and allowed the application of the fluorescence lifetime to monitor the interaction process. However, this approach does not have the capability to post process on shorter timescales than selected in the initial measurement conditions and is limited to one detection channel. We have previously used the “time-tag” or “photon streaming” technique to monitor the gelation process in sol-gel derived media via viscosity sensitive fluorescent dyes [21]. This method of data collection involves the “time stamping” of the individual photon arrival times; in terms of macrotime (relative to the start of the experiment)

and microtime (relative to the excitation pulse). This provides a wealth of data at the expense of generating large data files. Its time-resolution is limited by the macrotime clock and it is also capable of being used for dual channel data collection. Thus, it is applicable as a means to monitor the two principal wavelength bands emanating from the CT extract simultaneously at a good time resolution.

The photon streaming experiment involved the addition (with stirring at 37 °C) of 100 μL of 37.5 mg/mL of α-amylase solution to 2 mL of the CT extract (i.e. ~1.9 mg / mL of enzyme) and the system monitored for approximately half an hour. It was estimated that this would ensure an equivalence or excess of enzyme to facilitate the observation of CT extract binding and at a concentration ratio slightly less (for the CT extract) than that used in the inhibition study [11]. A measurement of the instrumental response function (IRF) was taken for both of the detection channels for use in the data analysis prior to the streaming measurement. The relative change in fluorescence intensity at both wavelengths during the course of the experiment is shown in Fig. 3. An increase in the relative intensity of the fluorescence monitored at 485 nm is clearly visible on the addition of enzyme, (in region between 10 and 20 seconds). Also, to a lesser extent, there is a decrease in the relative fluorescence intensity of the emission monitored at 655 nm. Thus it is evident that an interaction between the CT extract and the α-amylase has occurred. The data shown in Fig. 3 is plotted, with data (photon events) “binned” every 90 ms (i.e a resolution of 90 ms / point). However, with the photon streaming approach it is possible to post process and “zoom” into regions at a higher resolution. The time resolution per point is limited by the macrotime clock, in this case 3 MHz, which corresponds to a minimum time per point of ~333 ns. The inset in Fig.3 shows the enzyme addition on a resolution of 0.5 ms per point. There is an obvious trade off, as there are fewer photon events per point at higher resolution and there will be a point at which there will be insufficient photon events to construct histograms to analyse lifetime data. It has been observed that close to 200 photon events are required to fit an exponential decay [22,27]. Thus, in order to fit the data, the number of photon events has to be taken into consideration and the resolution adjusted accordingly.

To analyse the time-resolved data a 20 second period was selected as a region of interest around the time of the enzyme addition. Histograms were constructed by binning the photon events from consecutive 5 ms time periods (i.e. giving a macrotime resolution of 5 ms / point) to obtain sufficient photons for lifetime analysis. For each emission wavelength, these 4000 decay histograms were then analysed globally as a sum of three exponential decay components. The outcome from this analysis is shown in Fig. 4. In comparison to the intensity data there are some interesting features to note. Although the data is “noisy” it is still possible to infer trends by fitting it. In principle it can be possible to further analyse the data by using techniques used in another area where there is a sparcity of photons, single-molecule measurements. An example would be to use a method based on a generalised likelyhood ratio test [28].However, the fact that we can change the time resolution per point (e.g. as seen in Fig

3 and Fig 4) gives confidence that a change is occuring in the CT emission upon addition of enzyme. We acknowledge that further analysis could be helpful since the average lifetime exhibits a different trend to the intensity data, however it is clear that an interaction is occurring and the data is capable of recovering relative differences between the two observed wavelengths. Considering the emission at 485 nm, where an increase in the fluorescence intensity was observed, the average fluorescence lifetime (calculated from eq. 4) of the CT extract. Fig. 4a shows a decrease in average lifetime upon addition of the enzyme and is accounted for by an increase in the contribution of a shorter-lived (174 ps) decay in comparison to the two longer-lived emissions. In the case of the longer wavelength (655 nm) emission, where the intensity data show a decrease upon enzyme addition, an increase in the average lifetime is observed. This relates to a relative decrease in the contribution of a 244 ps lifetime and an associated increase in the contribution of a 723 ps decay. Throughout the contribution of the longer-lived (2.3 ns) decay appears more or less constant.

More note worthy is the fact that there are apparently differences in the rates for the changes in the data between the two emission wavelengths. Fitting indicates that the interaction process, as sensed by the change in fluorescence, is about an order of magnitude faster (0.05 s^{-1} compared to 0.37 s^{-1}) when monitored at 485 nm as compared to 655 nm. This is indicative of different components of the CT extract interacting with the enzyme with different rates and is in keeping with interactions between bovine serum and an anthocyanin [29] and other flavonoids [30]. Those studies were also indicative that the interaction of the anthocyanin was also about an order of magnitude different to the shorter wavelength emitting flavonoids. It has been reported that for cyanidin-3-gluocide the binding to α-amylase has influence on the enzyme structure, which is reflected in the enzymatic activity [31]. Concerning the shorter wavelength emission, there are also reports involving rutin and quercetin which can emit in the shorter wavelength region [32]. These are pertinent to this work as they are components of the extract [15] and it has been found that quercetin has a stronger affinity to proteins than rutin [30,33]. This stronger affinity was also found in relation to α-amylase [34]. The quantum yield of quercetin can be very low in solution, but increases upon protein binding [35,36]. Our observation for the shorter wavelength emission (Fig. 3) is of an increase in fluorescence intensity upon addition of α-amylase, which is in keeping with an increase in quantum yield from going from aqueous solution to a more hydrophobic environment. Because the extract is a mixture of different species, it is acknowledged that it would difficult, and speculative, to make firm assignments of the lifetime components. Thus, for the purpose of this study, it is the relative changes that are of importance, as they will be indicative of the interaction process. However, it is interesting to note that protein bound rutin has been reported to exhibit lifetimes of 0.39 ns and 4.86 ns [33], while quercetin and its derivatives exhibit enviromentally sensitive lifetimes in the order of 5 ns and less [37,38].

To further investigate the CT extract - α-amylase interaction TRES measurements were made, both before and after the addition of the enzyme, and the decay associated spectra determined. These are shown in Fig. 5 and differences in the CT extract emission can be easily observed. The “short” decay associated spectra, obtained by fixing to a value of 13 ps to account for scatter and very short-lived species, is dominated by a narrow band. This band can be simply ascribed to a Raman scattering process. Throughout, as with the steady state, there are two main spectral features. One around 485 nm and the other at ~655 nm. These can be just about discerned in the “short” lifetime decay associated spectra, with a small relative increase in their amplitude in the presence of enzyme.

If we consider each wavelength region in turn for the CT extract, then for the shorter wavelength emission centred around 485 nm the main lifetime contributions are 4.8 ns and 0.8 ns. The former lifetime is the major contribution to the emission at this wavelength. The decay associated spectra in this spectral region in the presence of the α-amylase indicate that the fluorescence decay is now more complex. There is an appearent increase in the longer-lived decay (4.38 ns to 6.02 ns), where the 485 nm emission is the only spectral feature (Fig. 5). There is also an increase in the contribution of the other lifetime components in this spectral region. This is indicative of a change in the “fluorescent environment” brought about by the presence of the enzyme and is reflected in the lifetime values and their contribution to the overall fluorescence emission. Again because of the complexity of the CT extract, it is only really the change in the lifetime / spectral data that is important and we acknowledge that these data encompass a variety of different fluorescing species. In the longer wavelength spectral region around 655 nm (Fig. 5), which is dominated by anthocyanin emission, there is also a change in lifetimes. This is indicative of an interaction between the CT extract and the α-amylase. It is also clear (Fig. 5c), because of the spectral widths and peak positions, that the emission in this region originates from several different anthocyanins. Thus it is apparent that, although we have not separated individual compounds, a more complete picture of the interaction between the CT extract and α-amylase has been achieved by being able to monitor two classes of componds in the extract simultaneously and aided by the use of decay associated spectra.

4. Summary

In this work we have monitored the kinetics of the interaction of an extract from *Clitoria ternatea* (CT) with a digestive enzyme, α-amylase, using time-resolved fluorescence techniques. The CT extract was found to inhibit the enzyme activity and when using 392 nm to excite the CT extract, two principal fluorescence emission bands were observed. Each band exhibited a different average fluorescence lifetime. The longer wavelength band most likely relates to anthocyanin emission, while that at shorter wavelengths may originate from other

flavonoids. Monitoring the CT extract simultaneously at both 485 nm and 655 nm elucidated changes in both fluorescence intensity and lifetime upon addition of α-amylase. This was related to the interaction (binding) of components of the extact to the enzyme. The change in fluorescence monitored at the shorter wavelength occurred about an order of magnitude faster than that at the longer wavelength. This is indicative of different binding rates for anthocyanins and other flavonoids present. The use of photon streaming enabled time-resolved fluorescence to be applied to this kinetic study and is well suited in elucidating information concerning the interaction between the extract and enzyme leading to its inhibition.

References

[1] WHO. Global Report on Diabetes 2016 [online] http://www.who.int/diabetes/global-report/en/ (Accessed on 4 April 2017).

[2] M. Türkyilmaz, O. Yemiş, M. Őzkan. Food Chem., 134 (2012) 1052-1058.

[3] M.L Castro-Acosta, L. Smith, R.J. Miller, D.I. McCarthy, J.A. Farrimond, W.L. Hall. J. Nutr. Biochem., 38 (2016) 154.

[4] G. Camelo-Méndez, E. Agama-Acevedo, M.M. Sanchez-Rivera, L.A. Bello-Pérez. Food Chem., 211 (2016) 281.

[5] L.E. Rojo, D. Ribnicky, S. Logendra, A. Poulev, P. Rojas-Silva, P. Kuhn, R. Dorn, M.H. Grace, M.A. Lila, I. Raskin. Food Chem., 131 (2012) 387.

[6] S. Kumar, S. Chakravarty. Amylases. In: Enzymes in Human and Animal Nutrition. Academic Press, Cambridge, US, 2018, pp.163-180.

[7] D.J. Vocadlo, G.J. Davies. Curr. Opinion Chem. Biol., 12 (2008) 539.

[8] Y. Kim, J.B. Keogh, P.M. Clifton. Nutrients, 8 (2016) 17.

[9] A. Lovegrove, C.H. Edwards, I. de Noni, H. Patel, S.N. El, T. Grassby, C. Zielke, M. Ulmius, L. Nilsson, P.J. Butterworth, P.R. Ellis, P.R. Shewry. Crit. Rev. Food Sci. Nutr., 57 (2017) 237.

[10] J. Xiao, X. Ni, G. Kai, X. Chen. Crit. Rev. Food Sci. Nutr., 53 (2013) 497.

[11] B.-S.Chu, R. Divers, A. Tziboula-Clarke, M.A. Lemos. Am. Res. J. Food Nutr., 1 (2017) 1.

[12] T. Goto, T. Kondo. Angew Chem Int Ed English, 30 (1991) 17.

[13] M.F. Mohamad, S.N.S Nasir, M.R. Sarmidi. Asian Journal of Food Agro-Industry. 4 (2011) 306.

[14] N. Terahara, M. Oda. J. Nat. Prod., 59 (1996) 139.

[15] V. Nair, W.Y. Bang, E. Schreckinger, N. Andarwulan, L. Cisneros-Zevallos. J. Agric. Food Chem., 63 (2015) 6355.

[16] K. Kamzuma, N. Noda, M. Suzuki. Phytochem., 62 (2003) 229.

[17] K. Kamzuma, K. Kogawa, N. Noda, N. Kato, M. Suzuki. Chem. Biodivers., 1 (2004) 1762.

[18] K. Kamzuma, N. Noda, M. Suzuki. Phytochem., 64 (2003) 1133.

[19] B. Anthika, S.P. Kusumocahyo, H. Sutanto. Procedia Chem., 16 (2015) 237.

[20] Lakowicz, J.R. Principles of Fluorescence Spectroscopy, 3rd Ed. Springer, New York, **2006**.

[21] G. Hungerford, A. Allison, D. McLoskey, M.K. Kuimova, G. Yahioglu, K. Suhling. J. Phys. Chem. B, 113 (2009) 12067.

[22] M. Köllner, J. Wolfrum. Chem. Phys. Lett., 200 (1992) 199.

[23] D.J.S Birch, R.E Imhof. *Time-domain fluorescence spectroscopy using time-correlated single photon counting* in Topics in Fluorescence Spectroscopy vol 1: Techniques, Lakowicz, J.R. (ed), Plenum Press, New York , 1991, pp 1-95.

[24] M.A. Lemos, G. Hungerford. Photochem. Photobiol., 89 (2013) 1071.

[25] B. Valeur, Molecular Fluorescence: Principles and Applications, Wiley-VCH, New York, **2002**.

[26] M.A. Lemos, K. Sárniková, F. Bot, M. Anese, G. Hungerford. Biosensors, 5 (2015) 367.

[27] D. McLoskey, D. Campbell, A. Allison, G. Hungerford. Meas. Sci. Technol., 22 (2011) 067001.

[28] L.P. Watkins, H. Yang. J. Phys. Chem. B. 109 (2005) 617.

[29] T. Lin, L. Shu, B. Honga, G. Xin. Food Chem., 196 (2016) 550.

[30] A. Papadopoulou, R.J. Green, R.A. Frazier. J. Agric. Food Chem., 53 (2005) 158.

[31] S. Wiese, S. Gärtner, H.M. Rawel, P. Winterhalter, S.E. Kulling. J. Sci. Food Agric., 89 (2008) 33.

[32] E. Sudo, M. Teranishi, J. Hidema, T. Taniuchi. Biosci. Biotechnol. Biochem., 79 (2009) 2107.

[33] A.V. Pastukhov, L.A. Levchenko, A.P. Sadkov. J. Mol. Struct, 842 (2007) 60.

[34] Y. Li, F. Gao, F. Gao, F. Shan, J. Bian, C. Zhao. J. Food Sci., 74 (2009) C199.

[35] M. Poór, G. Broda, S. Kunsági-Máté, P.W. Needs, P.A. Koon, B. Lemli. J. Luminescence, 194 (2018) 156.

[36] A. Mezzeti, S. Protti, C. Lapouge, J.-P. Conard. Phys. Chem. Chem. Phys., 13 (2011) 6858.

[37] H.-R. Park, Y. Daun, J.K. Park, K.-M. Bark, Bull. Korean Chem. Soc., 34 (2013) 211.

[38] H.-B. Liu, D. Yu, S.C. Shin, H.-R. Park, J.K. Park, K.-M. Bark. Photochem. Photobiol., 85 (2009) 934.

Figure captions

Fig 1. (**a**) Steady state absorption (blue) and emission (red) spectra for the CT extract. The excitation wavelength was 392 nm and the spectra are shown normalised. (**b**) time resolved fluorescence decays monitored at 485 nm and 655 nm, with the excitation at 392 nm. A representative instrumental response function (IRF) is also shown along with an indication of the average lifetime.

Fig 2. Inhibition of α-amylase activity and concentration of liberated glucose with the addition of the CT extract to the enzyme.

Fig 3. Change in fluorescence intensity (from a photon streaming measurement) of the CT extract with the addition of α-amylase. The fluorescence was excited at 392 nm and the emission monitored at 485 nm and 655 nm simultaneously. The graph displays a resolution of 90 ms per point. The inset shows the region of α-amylase at a resolution of 500 μs per point. Note the time axis is shown on a log scale.

Fig 4. Change in the average fluorescence lifetime (**a** & **c**) from a photon streaming measurement) of the CT extract with the addition of α-amylase. The fluorescence was excited at 392 nm and the emission monitored at 485 nm and 655 nm simultaneously. Data were analysed as the sum of three exponential decays in a global analysis. (**b** & **d**) show the trends in the respective normalised pre-exponential components. The fit lines are shown for guidance purposes.

Fig 5. Decay associated spectra for the CT extract, (**a**) before and (**b**) after the addition of α-amylase. These are shown normalised in (**c**) for the CT extract and (**d**) for the CT extract – enzyme mixture.

Graphical abstract

Binding of *C. ternatea* extract to α-amylase followed using time-resolved fluorescence monitoring 2 wavelengths simultaneously using a photon streaming approach

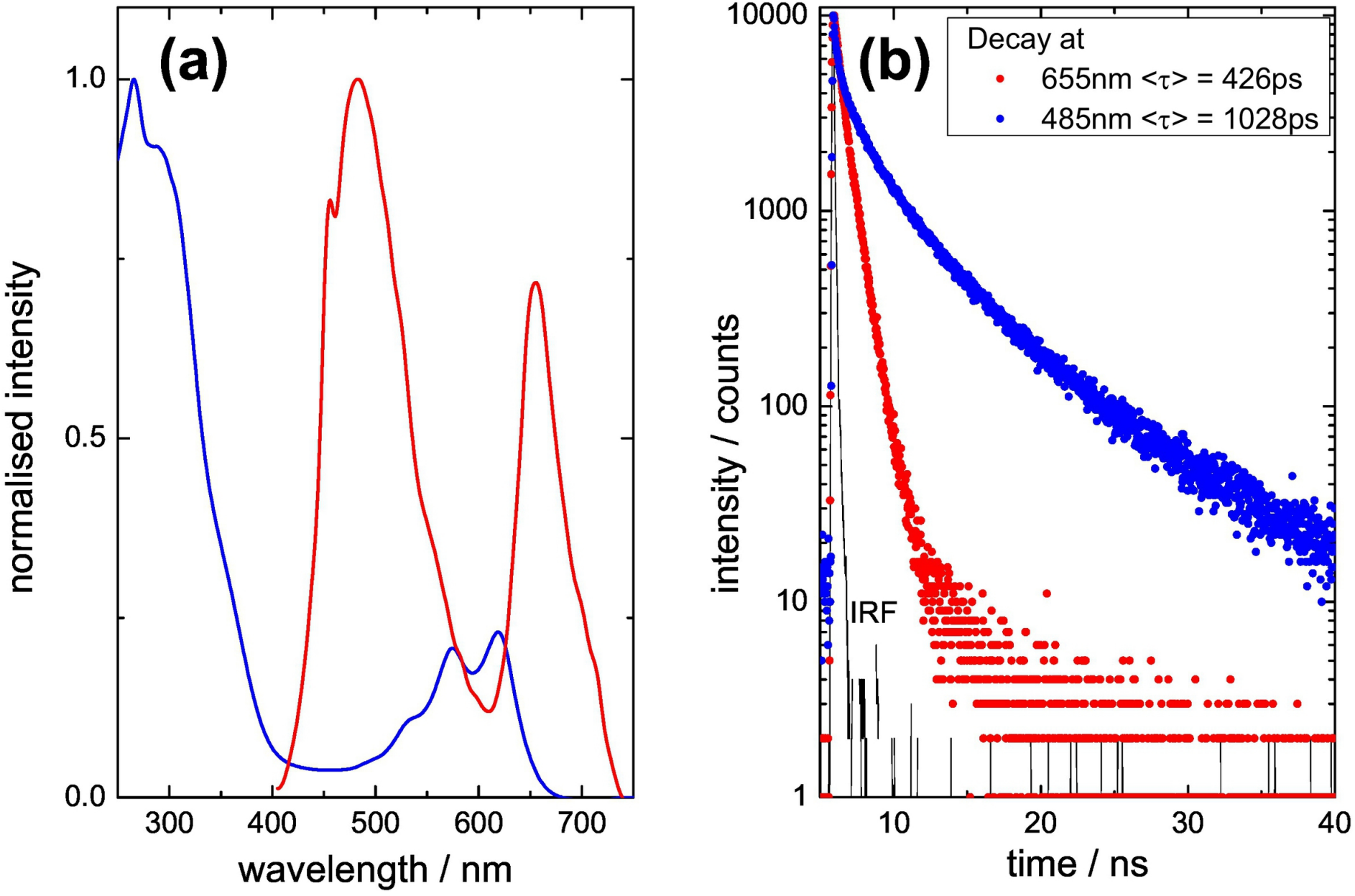
(a)
normalised intensity
1.0
0.5
0.0
300
400
500
600
700
wavelength / nm
(b)
Decay at
655nm <τ> = 426ps
485nm <τ> = 1028ps
IRF
intensity / counts
10000
1000
100
10
1
10
20
30
40
time / ns

Figure 1

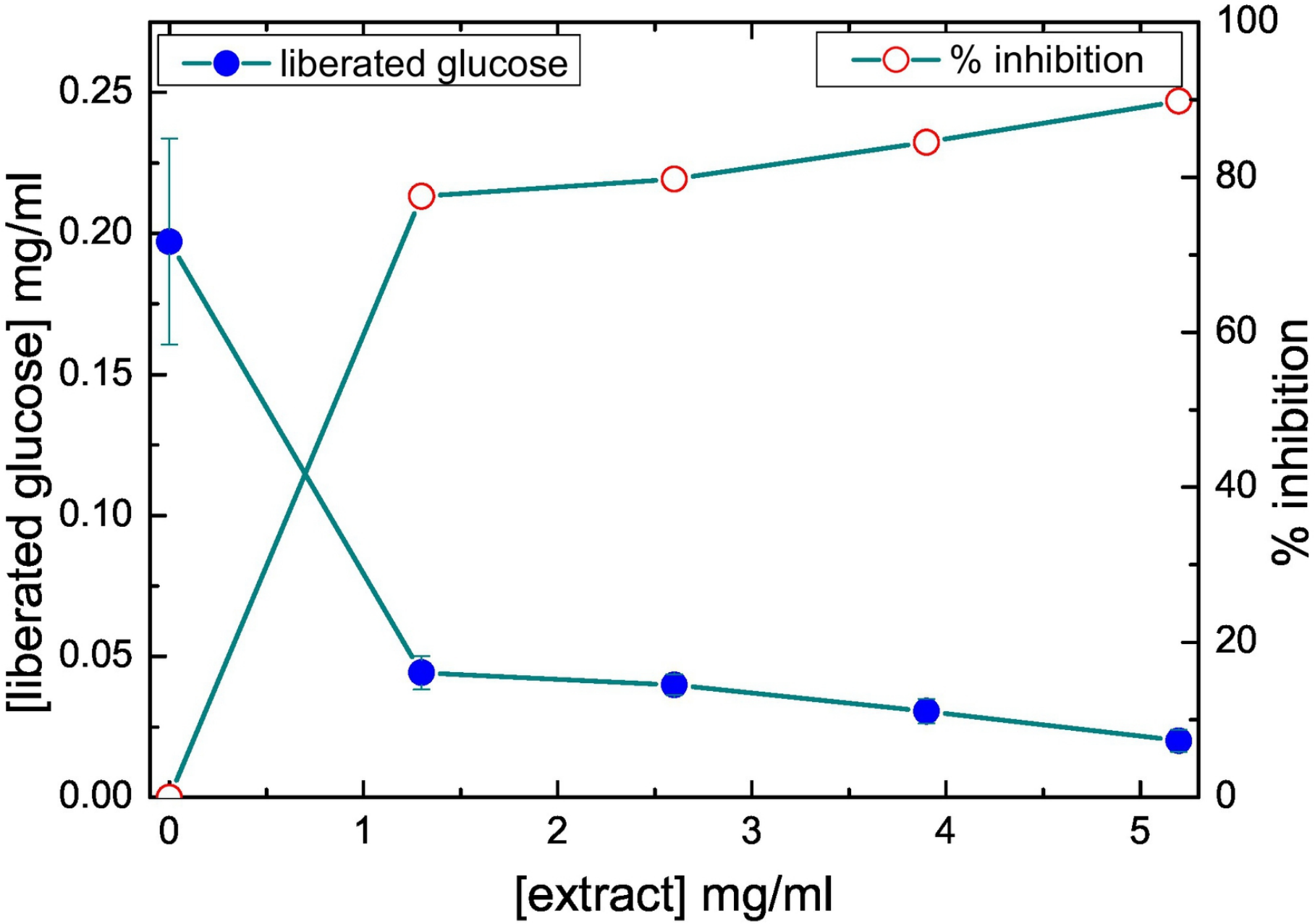
liberated glucose
% inhibition
[liberated glucose] mg/ml
% inhibition
[extract] mg/ml
0.00
0.05
0.10
0.15
0.20
0.25
0
20
40
60
80
100
0
1
2
3
4
5

Figure 2

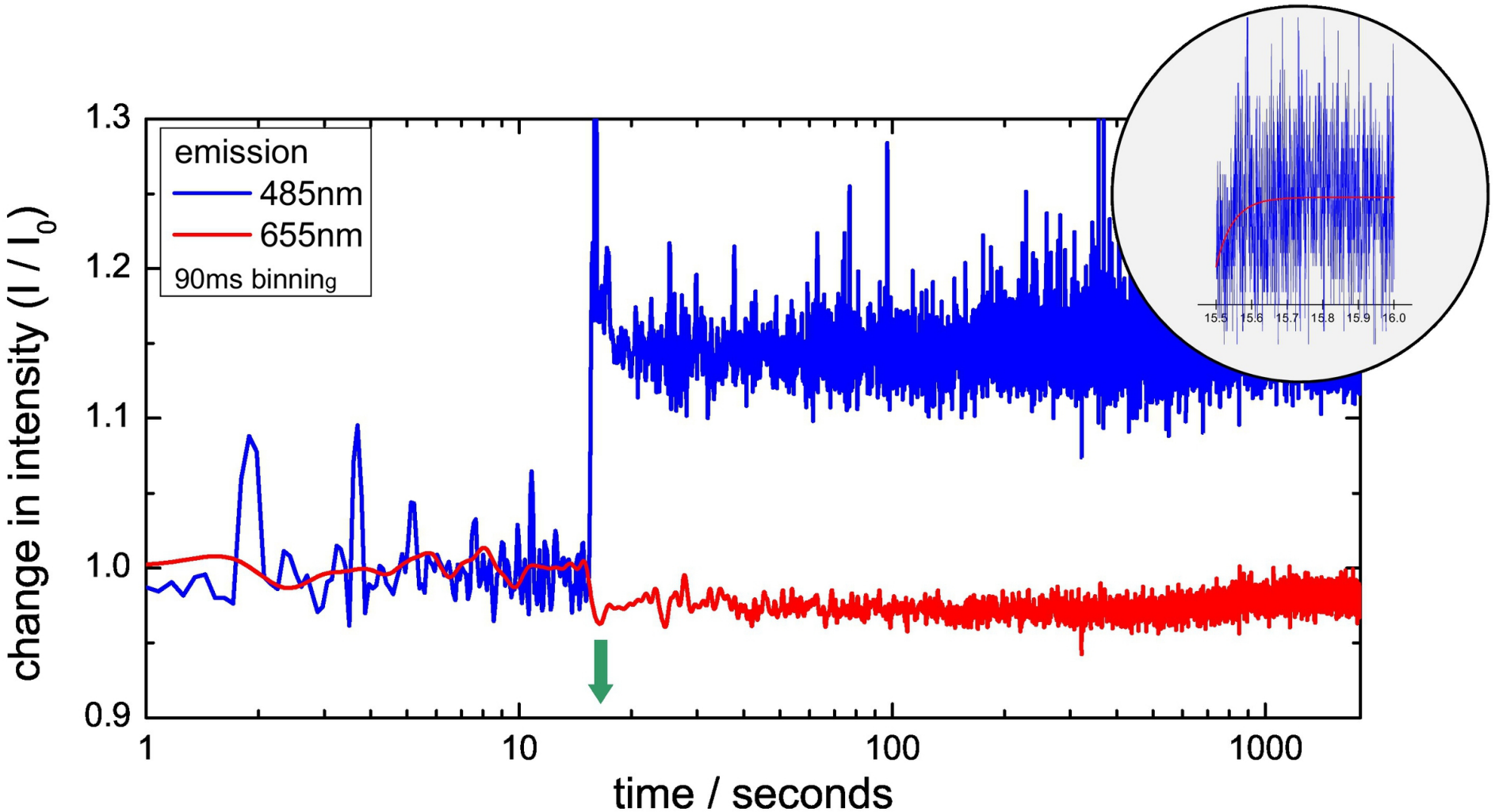
emission
485nm
655nm
90ms binning
change in intensity (I / I0)
time / seconds
1.3
1.2
1.1
1.0
0.9
1
10
100
1000
15.5
15.6
15.7
15.8
15.9
16.0

Figure 3

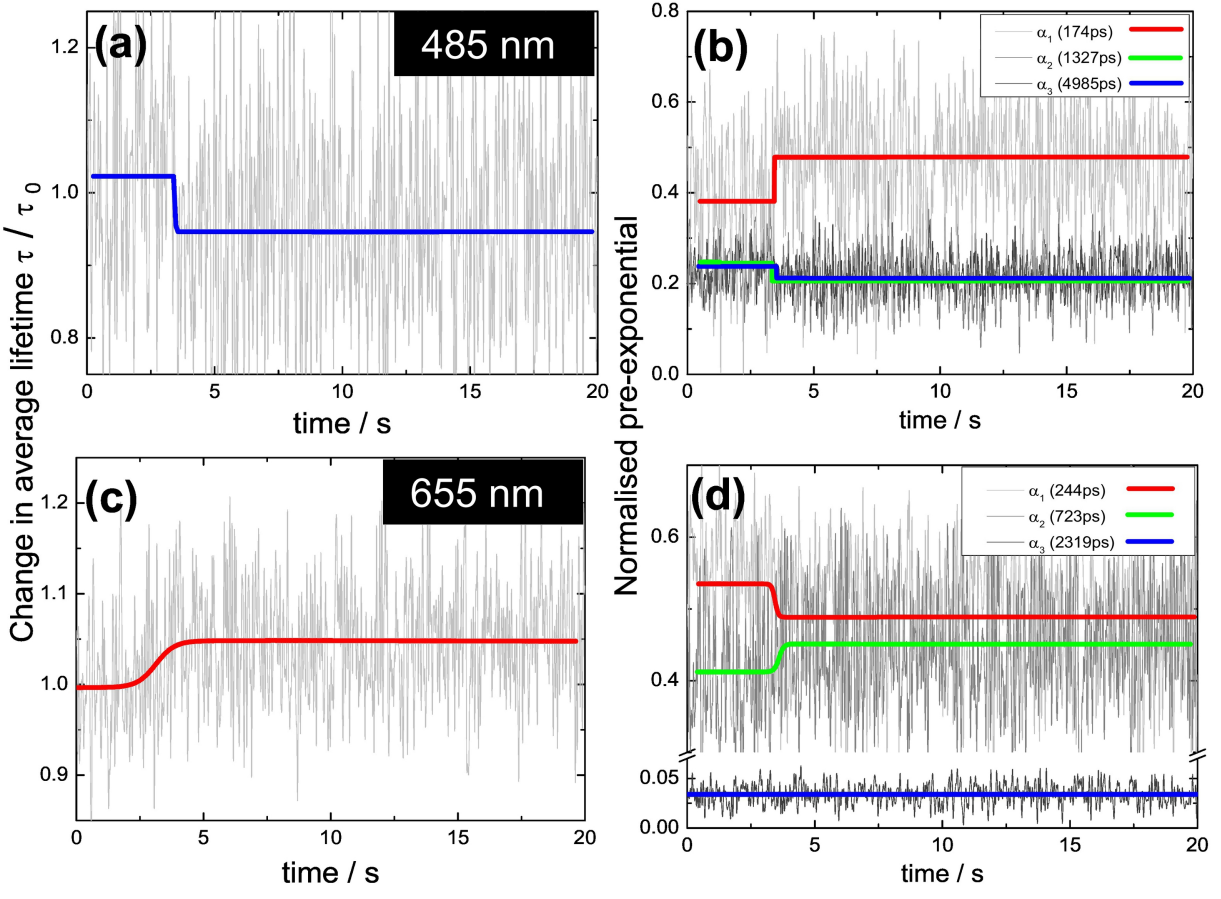
(a)
485 nm
Change in average lifetime τ / τ 0
time / s
(b)
α1 (174ps)
α2 (1327ps)
α3 (4985ps)
Normalised pre-exponential
time / s
(c)
655 nm
Change in average lifetime τ / τ 0
time / s
(d)
α1 (244ps)
α2 (723ps)
α3 (2319ps)
Normalised pre-exponential
time / s

Figure 4

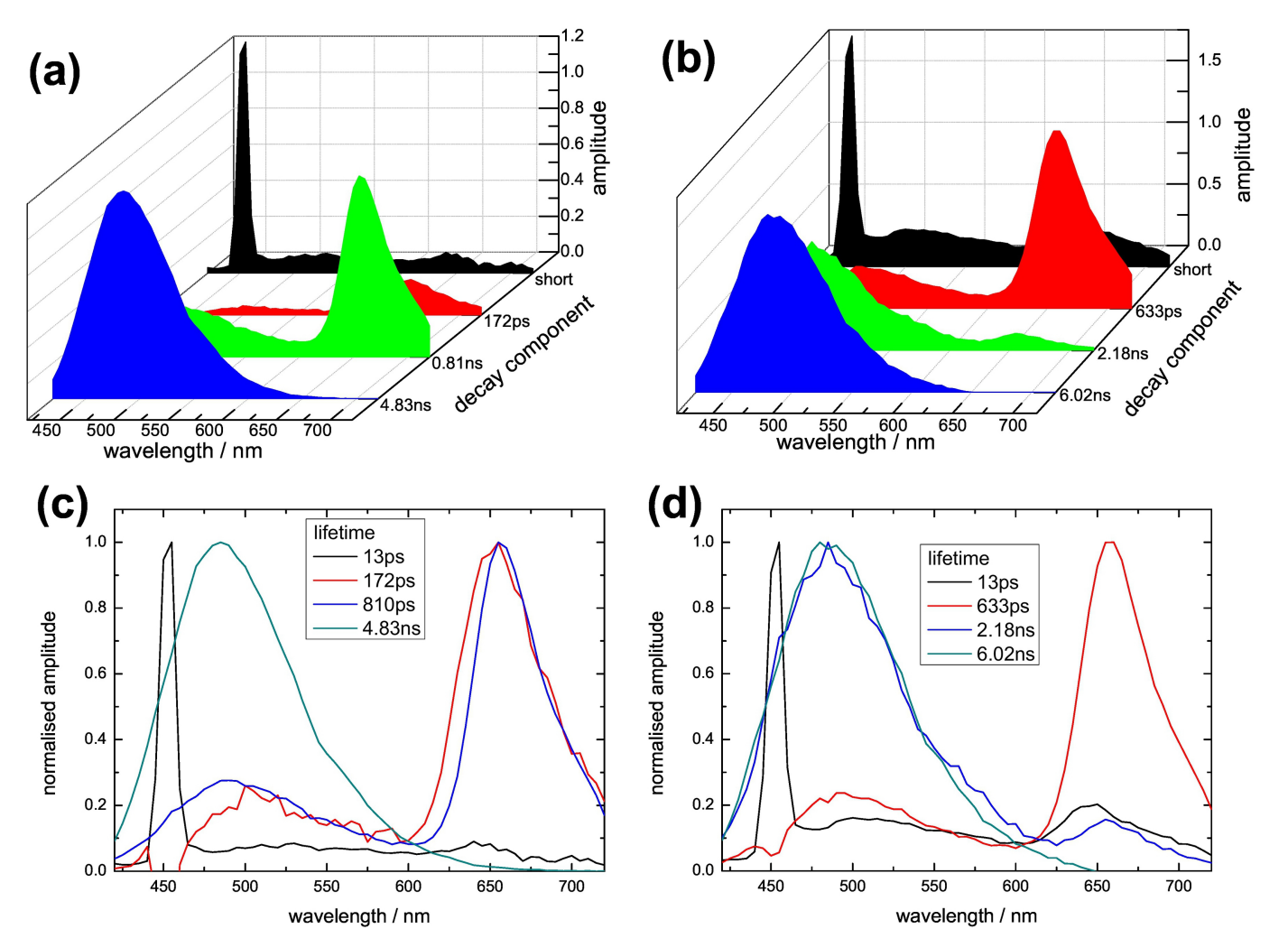
(a)
amplitude
short
172ps
0.81ns
4.83ns
decay component
wavelength / nm
(b)
amplitude
short
633ps
2.18ns
6.02ns
decay component
wavelength / nm
(c)
lifetime
13ps
172ps
810ps
4.83ns
normalised amplitude
wavelength / nm
(d)
lifetime
13ps
633ps
2.18ns
6.02ns
normalised amplitude
wavelength / nm

Figure 5